

Prediction model of form error influenced by grinding wheel wear in grinding process of large-scale aspheric surface with SiC ceramics

Lifei Liu¹ · Feihu Zhang²

Received: 4 December 2015 / Accepted: 25 April 2016 / Published online: 2 May 2016
© Springer-Verlag London 2016

Abstract Because of the material characteristic of high hardness and high abrasion resistance of SiC ceramics, grinding wheel wear is an essential problem which must be taken seriously and be solved in grinding process, especially in grinding of large-scale aspheric surface. In this paper, a ground aspheric surface form error model in large-scale aspheric surface grinding process of SiC ceramics is built without considering any other conditions but just radius wear of the grinding wheel. In this model, volume grinding ratio is employed to combine the wear volume of the grinding wheel and the removed volume of SiC ceramics. Experiments are conducted to corroborate the feasibility of the model, and the results reveal that the forecast error between the predicted value and the experimental value is less than 15 %. Considering the assumptions and interference of other factors, the form error model is acceptable.

Keywords Grinding wheel wear · SiC ceramics · Aspheric surface · Form error · Modeling

Nomenclature

a_p	Grinding depth, μm
v_s	Grinding speed, m/s
f_s	Feed rate, mm/min
R	Basic radius of grinding wheel
r	Arc radius of grinding wheel

θ_x	Angle between the center axis of grinding wheel and the connecting line between arc center of grinding wheel and wheel-workpiece contact point
G	Grinding ratio
α	Inclination angle between wheel rotary axis and the horizontal axis
β_x	Tangent angle on the generator of aspheric surface
r_0	Paraxial curvature radius of aspheric surface
e	Eccentricity of aspheric surface

1 Introduction

SiC ceramics has material characteristics such as high specific stiffness, low density, small thermal deformation coefficient, and good dimensional stability. All these characters make it an ideal material for manufacturing of optical reflectors and getting more and more attention and application in satellites, defense, space telescopes, and other fields [1–3]. While due to the serious grinding wheel wear, the poor machining quality and low processing efficiency are the main challenges in manufacturing of SiC reflectors which researchers must face [4–6].

A considerable number of studies have been implemented in order to decrease the form error and subsurface damage of aspheric surface. Researches mainly put their focus on form error after polishing, optimization of machining path, material removal rate, machining forces, qualitative analysis of grinding wheel wear, and so on [7–11]. While studies related to form error affected by grinding wheel wear in grinding process of SiC ceramics are limited, Gupta et al. [12] carried out studies on Nickel-silicon-chromium-copper (C18000) with single-point diamond turning operation to minimize the profile error, and found that feed rate plays the most significant role in minimizing of profile error and followed by nose radius

✉ Lifei Liu
liulf_87@163.com

¹ Harbin University of Science and Technology, Harbin, China

² School of Mechatronics Engineering, Harbin Institute of Technology, Harbin, China

and spindle speed. Cao et al. [13] studied the advantages of ultrasonic-assisted internal grinding (UAIG) on machining of SiC ceramics experimentally, and the experimental results indicated that the grinding forces in UAIG are reduced obviously. Meanwhile, they also found that the surface roughness and sub-surface damages are decreased by a wide margin. Chen et al. [14] employed a compensation method of single-point inclined axis nano-grinding, with tungsten carbide inserted to compensate the radius error of grinding wheel, and the finished form error was obtained by 200 nm in P-V value. Cheng et al. [15] utilized magnetorheological finishing process to achieve high-precision aspheric mirrors, and a polishing wheel was employed combining self-rotation movement with corotation. A parabolic SiC mirror was obtained with figure accuracy of $\lambda/30$ rms. Chen et al. [16] analyzed the advantages of cross grinding mode against parallel grinding mode, and gained low surface roughness, high form accuracy by grinding experiments of aspheric surface.

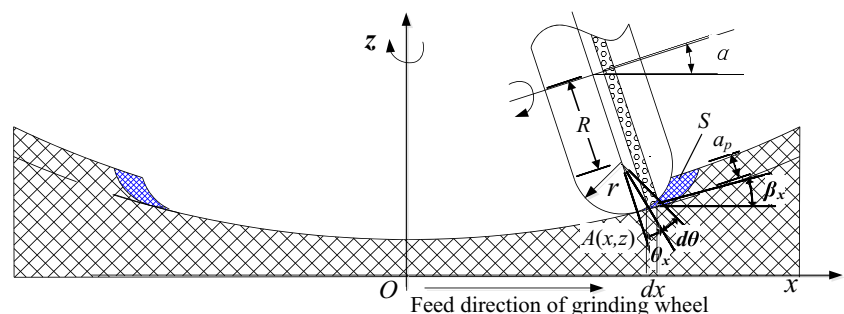
All these analyses of former literatures show that there are few studies of aspheric surface form error relating to grinding process of SiC ceramics, especially with the influence of radius and form wear of grinding wheel. In this paper, the expression of radius wear value of grinding wheel is given according to the grinding ratio between removed volume of SiC ceramics and wear volume of grinding wheel. And aspheric surface form error model is built based on the radius wear of grinding wheel, with the influence factors of grinding parameters, shape parameters of grinding wheel, shape parameters of aspheric surface, and so on. Finally, grinding experiments of aspheric surface on SiC ceramics are conducted to prove the form error model.

2 Model assumptions

The purpose of this paper is to build a model of grinding aspheric surface form error not considering any other parameters but the radius wear of metal bonded diamond grinding wheel. And grinding ratio is used as connection tools. So the following assumptions are needed:

Firstly, suppose that there are equal numbers of diamond abrasives and the abrasives are evenly distributed on each grinding wheel layer.

Fig. 1 Relationship of grinding wheel radius wear and material removed volume



Secondly, suppose that the diamond grinding wheel stay in a stable abrasion stage in grinding process of large-scale SiC ceramics aspheric surface, and there are no large range of grain crushing and block off.

Thirdly, suppose that the grinding ratio remains constant in stable grinding stage and is only determined by grinding processing parameters, as the grinding wheel parameters, material characteristic, grinding environments, etc. being determined.

Fourthly, suppose that only the radius wear of grinding wheel is considered in this model, and influence of other factors such as grinding tool precision, grinding environments, motional error, and so on are ignored.

The prediction model of aspheric surface form error is built based on the above four assumptions, with the purpose to reveal the influence of radius wear of grinding wheel on aspheric surface form error in grinding of SiC ceramics aspheric surface.

3 Modeling of form error in aspheric surface grinding of SiC ceramics

According to grinding principle, the grinding ratio means the specific value between wear volume of grinding wheel and removal volume of SiC ceramics, and it keeps constant in stable grinding stage. Therefore, the reduction amount of grinding wheel radius can be expressed with removal volume of SiC ceramics by grinding ratio and geometric relationships.

3.1 Reduction of grinding wheel radius

In this paper, parallel grinding method with arc diamond grinding wheel is utilized in grinding process. The basic radius of grinding wheel is R , with an arc radius of r , and the aspheric surface is a quadratic revolution aspheric surface. The inclination angle between wheel rotary axis and the horizontal axis is α . The workpiece coordinate system xoz of aspheric surface is established, as shown in Fig. 1. When wheel-workpiece contact point moved to a point $A(x, z)$ on generator line of aspheric surface, the angle between the center axis of grinding wheel and the connecting line between arc center of grinding wheel and wheel-workpiece contact point is considered as θ_x . The

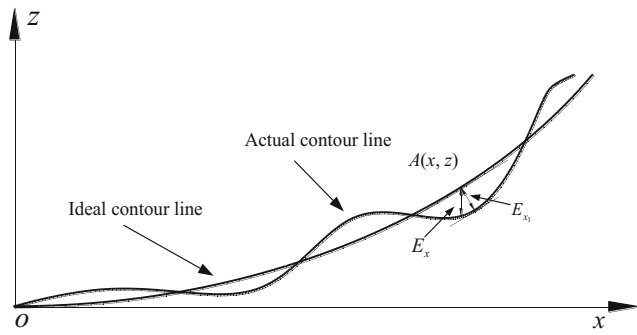


Fig. 2 Schematic diagram of aspheric surface form error

removal volume of SiC ceramics at this point is d_{V_w} . As the grinding wheel moving along the positive direction by a distance of d_x , its cross-sectional area of the removed volume of SiC ceramics is shown as S in Fig. 1. Then, the d_{V_w} can be expressed by the following equation:

$$d_{V_w} = 2\pi x \cdot (a_p - \Delta r_x) \cdot d_x \tag{1}$$

The micro-angle of wheel-workpiece contact point moved along grinding wheel arc can be represented as d_θ , as grinding wheel moved along positive direction of x on aspheric surface by d_x . So the wear volume of grinding wheel d_{V_s} , with a radius reduction amount of Δr_x , can be written as follows:

$$d_{V_s} = 2\pi(R + r) \cdot \Delta r_x \cdot r \cdot [\sin(\theta_x + d_\theta) - \sin\theta_x] \tag{2}$$

where $\theta_x \in (-\alpha, \beta_{x\max} - \alpha)$, $\beta_{x\max}$ means the max tangential angle on the meridian line of aspheric surface.

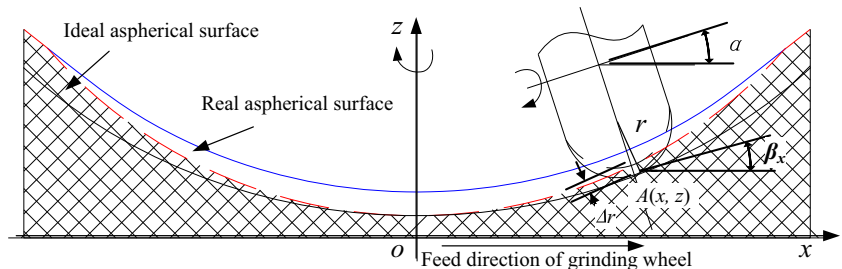
For the micro-increment of angle d_θ that wheel-workpiece contact point moves along grinding wheel arc, it can be known that $d_\theta \rightarrow 0$, according to its definition of infinitesimal. So that $\cos d_\theta \approx 1$ and $\sin d_\theta \approx d_\theta$. The equation $\sin(\theta_x + d_\theta)$ can be converted into the expression shown in Eq. (3), as the previously mentioned approximations being substitute into:

$$\begin{aligned} \sin(\theta_x + d_\theta) &= \sin\theta_x \cos d_\theta + \cos\theta_x \sin d_\theta \approx \sin\theta_x \\ &+ \cos\theta_x \cdot d_\theta \end{aligned} \tag{3}$$

Substituting Eq. (3) into Eq. (2), the wear volume of grinding wheel at the grinding point $A(x, z)$ can be written as follows:

$$d_{V_s} = 2\pi(R + r \cos\theta_x) \times \Delta r_x \times r \times \cos\theta_x \cdot d_\theta \tag{4}$$

Fig. 3 Influence of instantaneous wear of wheel radius on form error



In stable grinding stage, the grinding ratio G is approximately a constant value, and can be expressed as follows:

$$d_{V_w} = G d_{V_s} \tag{5}$$

Substituting the expression of removed volume of workpiece material, Eq. (2), and the wear volume of grinding wheel, Eq. (4), into Eq. (5), the following equation can be gained:

$$2\pi x \cdot (a_p - \Delta r_x) d_x = G \cdot 2\pi(R + r \cos\theta_x) \cdot \Delta r_x \cdot r \cdot \cos\theta_x d_\theta \tag{6}$$

Then, it can be simplified as follows:

$$x \cdot (a_p - \Delta r_x) d_x = G \cdot (R + r \cos\theta_x) \cdot \Delta r_x \cdot r \cdot d_\theta \cdot \cos\theta_x \tag{7}$$

From Eq. (7), the relationship between the micro-displacement feed amount d_x and the micro-angle feed amount d_θ can be expressed in the following equation:

$$\frac{d_x}{d_\theta} = \frac{G \cdot (R + r \cos\theta_x) \cdot \Delta r_x \cdot r \cdot \cos\theta_x}{x \cdot (a_p - \Delta r_x)} \tag{8}$$

In order to obtain the determinate relationship between Δr_x and other influence factors, the other expression of d_x/d_θ is needed.

Equation (9) shows the expression of the meridian line of the rotary aspheric surface. According to Eq. (9), the first derivative at point $A(x, z)$, namely the slope of tangent line, is written in Eq. (10):

$$z = \frac{x^2}{r_0 + \sqrt{r_0^2 - (1 - e^2)x^2}} \tag{9}$$

$$z'_x = \tan(\beta_x) = \tan(\theta_x + \alpha) = \frac{x}{\sqrt{r_0^2 - (1 - e^2)x^2}} \tag{10}$$

Taking the derivative of θ_x on both sides of Eq. (10), the following equation can be obtained:

$$\sec^2(\theta_x + \alpha) = \frac{r_0^2}{(r_0^2 - (1 - e^2)x^2)^{3/2}} \cdot \frac{d_x}{d_\theta} \tag{11}$$

According to the relationship between the trigonometric functions, the relative expressions of trigonometric function

$\cos(\theta_x + \alpha)$ and $\sin(\theta_x + \alpha)$ can be obtained by transforming of Eq. (10), which are shown as follows:

$$\cos(\theta_x + \alpha) = \frac{\sqrt{r_0^2 - (1 - e^2)x^2}}{\sqrt{r_0^2 + e^2x^2}} \tag{12}$$

$$\sin(\theta_x + \alpha) = \frac{x}{\sqrt{r_0^2 + e^2x^2}} \tag{13}$$

$$\sec^2(\theta_x + \alpha) = \frac{1}{\cos^2(\theta_x + \alpha)} = \frac{r_0^2 + e^2x^2}{r_0^2 - (1 - e^2)x^2} \tag{14}$$

Substituting Eq. (14) into Eq. (11), the relationship between d_x and d_θ can be expressed by another equation:

$$\frac{d_x}{d_\theta} = \frac{(r_0^2 + e^2x^2)\sqrt{r_0^2 - (1 - e^2)x^2}}{r_0^2} \tag{15}$$

Equation (16) can be generated by the simultaneous of Eqs. (8) and (15):

$$\frac{G \cdot (R + r \cos \theta_x) \cdot \Delta r_x \cdot r \cdot \cos \theta_x}{x \cdot a_p} = \frac{(r_0^2 + e^2x^2)\sqrt{r_0^2 - (1 - e^2)x^2}}{r_0^2} \tag{16}$$

From Eq. (16), it can be seen that all the factors have determinate expressions or values except Δr_x , so the radius wear of grinding wheel at any point $A(x, z)$ is obtained as follows:

$$\Delta r_x = \frac{a_p \cdot x (r_0^2 + e^2x^2) \sqrt{r_0^2 - (1 - e^2)x^2}}{r_0^2 \cdot G \cdot (R + r \cos \theta_x) \cdot r \cdot \cos \theta_x + x (r_0^2 + e^2x^2) \sqrt{r_0^2 - (1 - e^2)x^2}} \tag{17}$$

In Eq. (17), the expression of $\cos \theta_x$ can be deduced by Eqs. (12) and (13), as the value of the inclination angle α is determined. Expressions of $\cos(\theta_x + \alpha)$ and $\sin(\theta_x + \alpha)$ can be

presented by trigonometric of α and θ_x , and then be written as the following equations:

$$\begin{aligned} \cos(\theta_x + \alpha) &= \cos \theta_x \cdot \cos \alpha - \sin \theta_x \cdot \sin \alpha \\ &= \frac{\sqrt{r_0^2 - (1 - e^2)x^2}}{\sqrt{r_0^2 + e^2x^2}} \end{aligned} \tag{18}$$

$$\sin(\theta_x + \alpha) = \cos \theta_x \cdot \sin \alpha + \sin \theta_x \cdot \cos \alpha = \frac{x}{\sqrt{r_0^2 + e^2x^2}} \tag{19}$$

By considering Eqs. (18) and (19), the expression of $\cos \theta_x$ can be gained as follows:

$$\begin{aligned} \cos \theta_x &= \cos \alpha \cdot \cos(\theta_x + \alpha) + \sin \alpha \cdot \sin(\theta_x + \alpha) \\ &= \frac{\cos \alpha \sqrt{r_0^2 - (1 - e^2)x^2} + x \sin \alpha}{\sqrt{r_0^2 + e^2x^2}} \end{aligned} \tag{20}$$

Based on the above analysis, the radius wear at the grinding point $A(x, z)$ is given by Eq. (21), as grinding wheel feeding from rotary center to edge of aspheric surface in one grinding process.

$$\begin{cases} \Delta r_x = \frac{a_p \cdot x (r_0^2 + e^2x^2) \sqrt{r_0^2 - (1 - e^2)x^2}}{r_0^2 \cdot G \cdot (R + r \cos \theta_x) \cdot r \cdot \cos \theta_x + x (r_0^2 + e^2x^2) \sqrt{r_0^2 - (1 - e^2)x^2}} \\ \cos \theta_x = \frac{\cos \alpha \sqrt{r_0^2 - (1 - e^2)x^2} + x \sin \alpha}{\sqrt{r_0^2 + e^2x^2}} \end{cases} \tag{21}$$

As assumed in part 2, the grinding ratio G keeps constant in stable grinding stage, and just be determined by grinding parameters. So grinding experiments were carried out with precision grinding machine tool on SiC ceramics. The relative experimental data was obtained, and analysis had been done based on regression analysis method. The regression formulation of grinding ratio influenced by grinding parameters is generated as shown in Eqs. (22) and (21) and can be further expressed as Eq. (23).

$$G = 20.19857 \cdot v_s^{0.50252} \cdot a_p^{-0.064795} \cdot f^{-0.096309} \tag{22}$$

$$\begin{cases} \Delta r_x = \frac{a_p \cdot x (r_0^2 + e^2x^2) \sqrt{r_0^2 - (1 - e^2)x^2}}{20.19857 v_s^{0.50252} f^{-0.096309} a_p^{-0.064795} r_0^2 (R + r \cos \theta_x) \cos \theta_x + x (r_0^2 + e^2x^2) \sqrt{r_0^2 - (1 - e^2)x^2}} \\ \cos \theta_x = \frac{\cos \alpha \sqrt{r_0^2 - (1 - e^2)x^2} + x \sin \alpha}{\sqrt{r_0^2 + e^2x^2}} \end{cases} \tag{23}$$

Equation (23) reveals the wear amount of grinding wheel arc radius Δr_x at each point on generator of aspheric surface in stable grinding stage in grinding of SiC ceramics. It can be seen that the wear of arc radius is affected by grinding parameters, shape parameters of grinding wheel, and form

parameters of aspheric surface, and is different at a different wheel-workpiece contact point. In grinding of large-scale aspheric surface with SiC ceramics, the form error, which will be analyzed in next part, is mainly impacted by wear of arc radius Δr_x .

Table 1 Parameters of diamond grinding wheel

Diamond grain mesh number	Binding agent	Diameter of grinding wheel (mm)	Width of grinding wheel (mm)	Radius of grinding wheel arc (mm)	Length of handle (mm)	Diameter of handle (mm)	Dressing accuracy P-V (μm)
120#	Metal	40	16	20	80	20	11.9

3.2 Modeling of aspheric form error considering of wheel radius wear

There are different definitions of aspheric surface form error, as shown in Fig. 2. The E_x means the longitudinal distance and the E_{x1} means the normal distance of relative point between the ideal contour and the actual contour of aspheric surface. In this paper, the longitudinal distance E_x is chosen to delimit the form error of the aspheric surface, considering the convenience of detecting and data processing on aspheric surface.

Arc diamond grinding wheel is employed in the grinding of aspheric surface. The ideal arc radius of the grinding wheel is r after dressing process, and the radius wear is considered as Δr_x

at wheel-workpiece contact point $A(x, z)$, which can be calculated by Eq. (23). Therefore, the form error in longitudinal direction, E_x , can be gained by the geometric relationships with Δr_x and β_x , as shown in Fig. 3.

According to the former analysis and the geometric relationships shown in Fig. 3, form error of the grinding aspheric surface can be written in Eq. (24):

$$E_x = \frac{\Delta r_x}{\cos(\theta_x + \alpha)} \tag{24}$$

Substituting Eq. (23) into Eq. (24), the expression of form error E_x can be rewritten as follows:

$$\begin{cases} E_x = \frac{a_p \cdot x (r_0^2 + e^2 x^2)^{1.5}}{20.19857 v_s^{0.50252} f^{-0.096309} a_p^{-0.064795} r r_0^2 (R + r \cos \theta_x) \cos \theta_x + x (r_0^2 + e^2 x^2) \sqrt{r_0^2 - (1 - e^2) x^2}} \\ \cos \theta_x = \frac{\cos \alpha \sqrt{r_0^2 - (1 - e^2) x^2} + x \sin \alpha}{\sqrt{r_0^2 + e^2 x^2}} \end{cases} \tag{25}$$

From the expression of Eqs. (21) and (25), it is known that the form error of grinding aspheric surface is mainly determined grinding parameters of grinding depth, feed rate, and linear velocity of grinding wheel, as they directly affecting the grinding ratio.

4 Grinding experiments of aspheric surface on SiC ceramics

A mathematical model of form error on aspheric surface is built in part 3 based on grinding wheel wear. From the model, it can be conducted that the form error is mainly determined by grinding parameters, as the geometric size of grinding wheel and form parameters of aspheric surface is given. The form error at each

contact point on generator line can be calculated by this model, and it can be used to predict the form error before grinding process so that the processing staff can do some pre-compensation. In addition, when the max form error is restricted, the model can be used to optimize the processing parameters and the geometric parameters of grinding wheel. While it must be confirmed that the model is available in the predicting of form error. Experiments are carried out to test and verify the feasibility of the form error predicting model.

4.1 Experimental scheme

Processing parameters The DMG Ultrasonic 70–5 machining center is employed to conduct the grinding experiments of aspheric surface with SiC ceramics using a parallel grinding method. Arc diamond grinding wheel is chosen and parame-

Table 2 Grinding process parameters

Parameters	Linear velocity of grinding wheel (m/s)	Spindle speed (r/min)	Feed rate (mm/min)	Grinding depth (mm)	Inclination angle of grinding wheel (°)
Value	16.75	8000	150	0.02	20

Table 3 Material characteristic of SiC ceramics

Material	Density (g/cm ³)	Fracture toughness (MPa m ^{1/2})	Elastic modulus (GPa)	Thermal expansion coefficient (×10 ⁻⁶ /K)	Thermal conductivity (1000°) (W/m K)
Pressureless sintered SiC	3.12	3.2	410	4.7	45

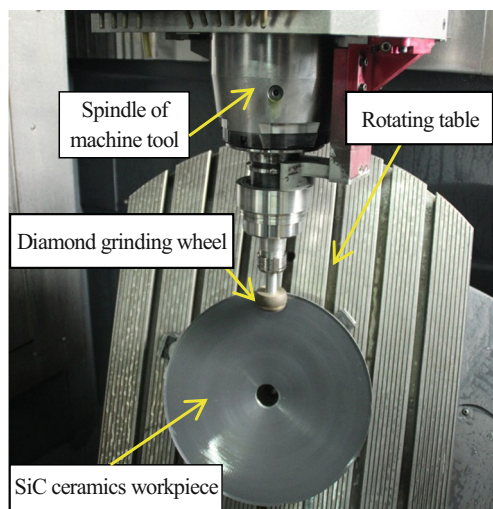
Table 4 Form parameters of aspheric surface

Equation of meridian line	Eccentricity ratio e	Paraxial curvature radius r_0 (mm)	Diameter of aspheric surface D (mm)
$z = x^2/900$	1	450	250

ters of grinding wheel is shown in Table 1. The grinding processing parameters are shown in Table 2 and the material characteristic of SiC is shown in Table 3. An aspheric surface with generatrix of parabola is designed and its form parameters are shown in Table 4 shows.

Clamping and positioning Positioning accuracy is an important factor of form error. In order to gain high positioning accuracy, a precise positing hole with diameter of $\Phi 30\text{mm}$ is designed in the center of SiC ceramics workpiece, which can be used to match the locating hole in rotary table of DMG machine tool. The positioning error of rotary centerline between the rotary table and the workpiece is less than $5\ \mu\text{m}$ with the minute adjustment by laser probe on machine tool. The processing status is shown in Fig. 4.

Detecting mode A graphite imprint method is utilized to record the grinding wheel shape before and after grinding process, and then the graphite imprints are detected by a profilometer to get the shape and dimension information of grinding wheel, from which the grinding wheel wear can be

**Fig. 4** Grinding mode of aspheric surface grinding

determined. The contour information of aspheric surface is obtained by a three-coordinate measuring machine and be analyzed to obtain the form error after grinding.

4.2 Results and discussion

4.2.1 Radius wear of grinding wheel

Figure 5a shows the aspheric surface of SiC ceramics after grinding, and Fig. 5b shows contradistinction of grinding wheel profile before and after grinding.

As the grinding wheel feeding from rotary center to the edge of aspheric surface, the corresponding central angle of wheel-workpiece contact arc on grinding wheel arc is 13.1° , calculated by Eq. (26). The value is determined by form parameters and diameter of aspheric surface.

$$\beta_{x_{\max}} = \arctan\left(\frac{x_{\max}}{\sqrt{r_0^2 + (1-e^2)x_{\max}^2}}\right) \quad (26)$$

As shown in Fig. 6, the blue mark and red mark mean the real profile of grinding wheel before and after grinding, while the dashed line and solid line are their fit lines, respectively. It can be seen that the radius in the left part of grinding wheel arc has been worn. The wear amount of radius at each point on

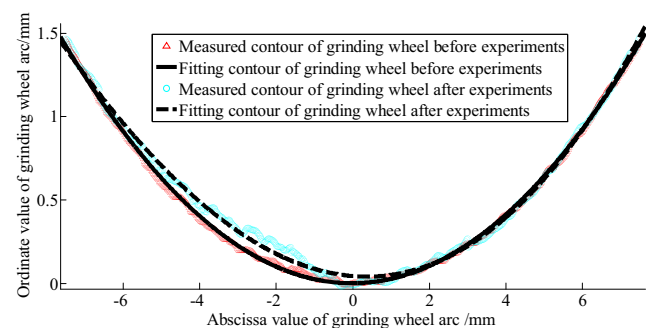
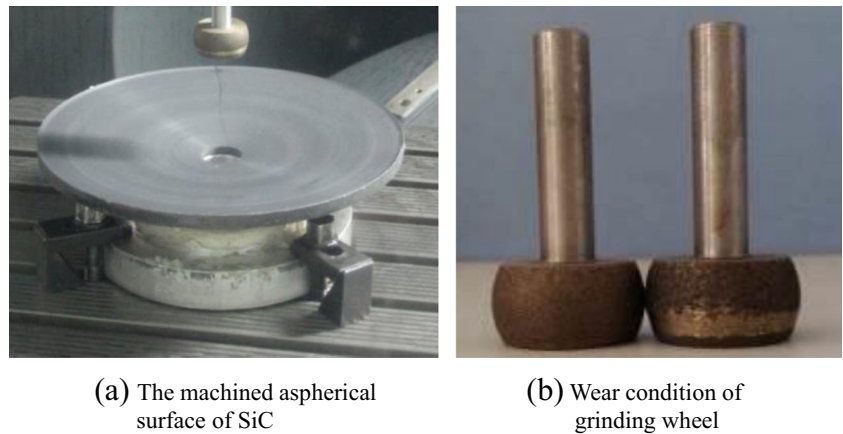
**Fig. 6** Fitting curves of profile contour of grinding wheel before and after experiments

Fig. 5 The aspheric surface and grinding wheel after experiments. **a** The machined aspherical surface of SiC. **b** Wear condition of grinding wheel



grinding wheel is calculated and is comprised with that predicted by radius wear model, shown in Eq. (23).

The normal distance at each contact point on grinding wheel is calculated and collected according the profile information shown in Fig. 6, which is considered as the experimental value of radius wear amount and is shown as red triangle mark in Fig. 7. The solid line in Fig. 7 is the fit line of experimental value. The dashed line in Fig. 7 is the predicted value of radius wear amount of grinding wheel. The percentage prediction error of radius wear amount can be calculated by Eq. (27).

$$E_x(\%) = \frac{E_{x-r} - E_{x-p}}{E_{x-r}} \times 100 \tag{27}$$

where E_{x-r} means the experimental value while the E_{x-p} means the prediction value.

According to experimental results and prediction results of radius wear shown in Fig. 7, it demonstrated that the change trend of experiment value is the same as prediction value, and the experimental value is larger than prediction value. The prediction errors are computed by Eq. (27), and the results reveal that the largest prediction error is less than 15 %. Considering of the assumptions in part 2 and the effecting of machine tool error, external grinding environment, grinding chatter, grinding force, grinding heat, and so on, the prediction

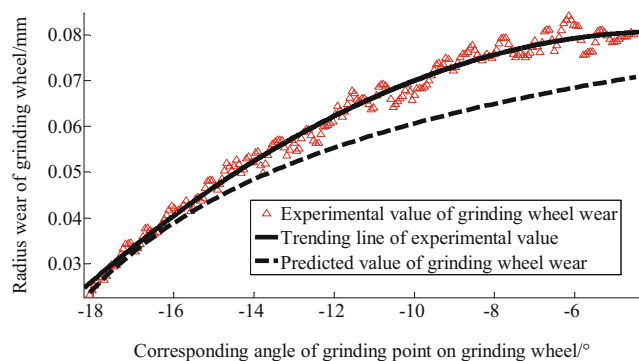


Fig. 7 Comparison of wheel radial wear of theoretical and experimental results

error is acceptable and Eq. (23) can be used to predict radius wear in grinding of SiC ceramics.

4.2.2 Form error of grinding aspheric surface

In order to obtain the profile information of the rotary aspheric surface, a three-dimensional coordinate system is built with the center of the center hole on aspheric surface being considered to be the origin point. The profile information in four generatrices on directions of 0°, 90°, 180°, and 270° are detected by a three-coordinate measuring machine, as shown in Fig. 8, and are counted and analyzed by mathematical software. Then, form errors of longitudinal error at the same x coordinate value between experimental value and prediction value are calculated. In order to minimize the effect of detection error, aspheric form errors on every two generatrices, 0° and 180°, 90° and 270°, are combined and took the average, also the average error of four generatrices is gained.

Figure 9 illustrated the prediction results and the experiment results of aspheric form error; it can be seen that both the experiment value and the prediction value have the same trends. The largest form error appears at the edge of aspheric surface, and the experiment value is larger than the prediction value. The percentage prediction error is calculated according to Eq. (27), and it can be seen that the largest error is less than 15 %. As the model is built only considering of the influence of radius wear, while there are other impact factors in grinding process that effect the form error, the prediction model of

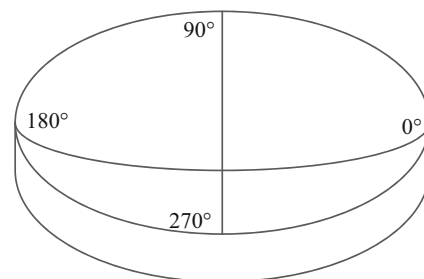


Fig. 8 Schematic diagram of aspheric contour detecting

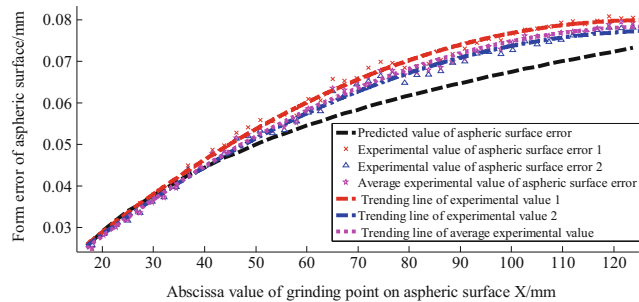


Fig. 9 Comparison of aspheric surface error of theoretical and experimental results

aspheric surface form error is available. It can be used to predict aspheric surface errors in the grinding process of SiC ceramics aspheric surface and provide guidance to reduce the form error in some extent.

5 Conclusions

The purpose of this paper is to build a model of aspheric form error only considering of the influence of radius wear in grinding of aspheric surface on SiC ceramics and verify its feasibility. Grinding ratio is utilized to connect the radius wear and removal volume of SiC ceramics. Then, the aspheric form error model is obtained according to the geometric relationship between form error and radius wear amount, with the influence of grinding parameters, shape parameters of grinding wheel, and aspheric surface. Metal-bonded diamond grinding wheel is chosen to conduct grinding experiments of aspheric surface with SiC ceramics on DMG machine tool. The experimental results indicate that the largest error between experiment value and prediction value is less than 15 %. Therefore, the prediction model of aspheric form error is available not considering any other conditions but radius wear of grinding wheel.

In this model, changes of grinding parameters and shape parameters of grinding wheel will impact from error obviously. So further research would be done later to reveal the influence of different parameters and process optimization of impact factors would be carried out to minimize the form error.

Acknowledgments This research was financially supported by the National Basic Research Program of China (973 Program, Grant No. 2011CB013202) and the National Natural Science Foundation of China (Grant No. 51175126).

References

1. Lightsey PA, Atkinson C, Clampin M (2012) James Webb space telescope: large deployable cryogenic telescope in space. *Opt Eng* 51(1):011003-1-011003-19.
2. Ji RJ, Liu YH, Zhang YZ, Cai BP, Li XP (2011) High-speed end electric discharge milling of silicon carbide ceramics. *Mater Manuf Process* 26(8):1050–1058
3. Shimizu Y, Goto S, Lee JC (2013) Fabrication of large-size SiC mirror with precision aspheric profile for artificial satellite. *Precis Eng* 37(3):640–649
4. Bhushan RK (2013) Multiresponse optimization of Al Alloy-SiC composite machining parameters for minimum tool wear and maximum metal removal rate. *J Manuf Sci Eng* 135(2):1–15
5. Demir H, Gullu A, Ciftci I, Seker U (2010) An investigation into the influences of grain size and grinding parameters on surface roughness and grinding forces when grinding. *SV-J Mech Eng* 56(7–8):447–454
6. Ni J, Li B (2012) Phase transformation in high-speed cylindrical grinding of SiC and its effects on residual stresses. *Mater Lett* 89: 150–152
7. Cao JG, Wu YB, Lu D, Fujimoto M, Nomura M (2014) Material removal behavior in ultrasonic-assisted scratching of SiC ceramics with a single diamond tool. *Int J Mach Tools Manuf* 79:49–61
8. Du J, Li J, Yao Y, Hao Z (2014) Prediction of cutting forces in mill-grinding SiCp/Al composites. *Mater Manuf Process* 29(3):314–320
9. Kuriyagawa T, Zahmaty MSS, Syoji K (1996) A new grinding method for aspheric ceramic mirrors. *J Mater Process Technol* 62(4):87–392
10. Bae HT, Choi HJ, Jeong JH, Lim DS (2010) The effect of reaction temperature on the tribological behavior of the surface modified silicon carbide by the carbide derived carbon process. *Mater Manuf Process* 25(5):345–349
11. Lin XH, Wang ZZ, Guo YB, Peng YF, Hu CL (2014) Research on the error analysis and compensation for the precision grinding of large aspheric mirror surface. *Int J Adv Manuf Technol* 71(1–4): 233–239
12. Gupta A, Ramagopal SV, Batish A, Bhattacharya A (2014) Surface roughness and profile error in precision diamond turning of C18000. *Mater Manuf Process* 29(5):606–613
13. Cao JG, Wu YB, Lu D, Fujimoto M, Nomura M (2014) Fundamental machining characteristics of ultrasonic assisted internal grinding of SiC ceramics. *Mater Manuf Process* 29(5):557–563
14. Chen F, Yin S, Ohmori H, Yu J (2013) Form error compensation in single-point inclined axis nanogrinding for small aspheric insert. *Int J Adv Manuf Technol* 65(1–4):433–441
15. Cheng H, Feng Z, Wang Y, Lei S (2005) Magnetorheological finishing of SiC aspheric mirrors. *Mater Manuf Process* 20(6): 917–931
16. Chen B, Guo B, Zhao Q (2015) An investigation into parallel and cross grinding of aspheric surface on monocrystal silicon. *Int J Adv Manuf Technol* 80:737–746, 1–10